

Adiabatic quantum pumping in graphene NIS junctions

M. Alos-Palop and M. Blaauboer

Kavli Institute of Nanoscience, Delft University of Technology, Lorentzweg 1, 2628 CJ Delft, The Netherlands

(Dated: February 16, 2022)

We investigate adiabatic quantum pumping through a normal metal-insulator-superconductor (NIS) junction in a monolayer of graphene. The pumped current is generated by periodic modulation of two gate voltages, applied to the insulating and superconducting regions respectively. In the bilinear response regime and in the limit of a thin high insulating barrier, we find that the presence of the superconductor enhances the pumped current per mode by a factor of 4 at resonance. Compared to the pumped current in an analogous semiconductor NIS junction, the resonances have a $\pi/2$ phase difference. We also predict experimentally distinguishable differences between the pumped current and the tunneling conductance in graphene NIS junctions.

PACS numbers: 72.80.Vp, 74.45+c, 73.23.-b

Adiabatic pumping is a transport mechanism in meso- and nanoscale devices by which a finite dc current is generated in the absence of an applied bias by low-frequency periodic modulations of at least two system parameters (typically gate voltages or magnetic fields) [1, 2]. In order for electrical transport to be adiabatic, the period of the oscillatory driving signals has to be much longer than the dwell time τ_{dwell} of the electrons in the system, $T = 2\pi\omega^{-1} \gg \tau_{\text{dwell}}$. Adiabatic *quantum* pumping [3] refers to pumping in open systems in which quantum-mechanical interference of electron waves occurs. In the last decade, many different aspects of quantum pumping have been investigated in a diverse range of nanodevices, for example charge and spin pumping in quantum dots [4], the relation of quantum pumping to geometric (Berry) phases [5] and the role of electron-electron interactions [6]. Quantum pumped currents have also been studied in hybrid systems consisting of normal-metal (N) and superconducting (S) parts, such as NS and SNS junctions [7–11]. Recently, investigations of quantum pumping in graphene mono- and bilayers have appeared [12].

In this Letter we investigate adiabatic charge pumping through a normal metal-insulating-superconductor (NIS) junction in graphene. The pumped current is generated by adiabatic variations of two gate voltages $U_0(t)$ and $V_0(t)$ which change, respectively, the Fermi level in the superconducting region and the height of the insulating tunnel barrier. The central question we aim to answer is what the effect of electron-hole (Andreev) reflection is on pumped charge currents in graphene. Using the scattering matrix formalism, we calculate the adiabatically pumped current at zero temperature in the linear response regime, i.e., for small variations of the pumping parameters U_0 and V_0 , and we compare this with the pumped current in the absence of the superconducting lead. Our main result is that the presence of the superconducting lead enhances the pumped current per mode by a factor of 4 and the total pumped current by a factor of $3\sqrt{2}/2$ at the resonant tunneling condition. Off resonance, the pumped current is an order of magnitude

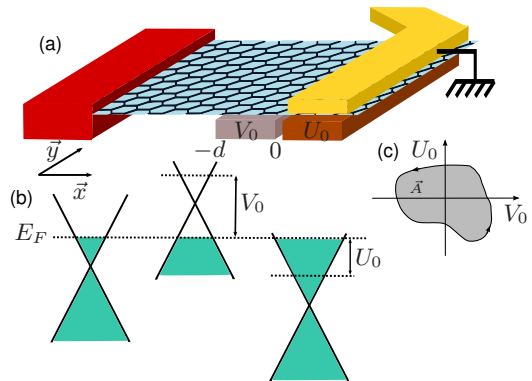


FIG. 1. (a) Sketch of the graphene NIS junction. The variable gate voltage V_0 creates the insulating barrier I of length d and the gate voltage U_0 is applied to the superconducting electrode (yellow). (b) Schematic of the energy levels in the three regions. (c) The area enclosed in the (U_0, V_0) parameter space during one pumping cycle.

smaller than the analogous current in a semiconductor NIS junction. We also find that whereas the conductance *increases* with U_0 for thin barriers, the pumped current *decreases* with U_0 . This difference might be used to discriminate between conductance and pumped currents in graphene NIS junctions. In the last part of the Letter, we briefly comment on the pumped current in the so-called specular reflection regime (where $\Delta_0 \geq E_F$ with Δ_0 the superconductor gap and E_F the Fermi energy) [13].

Consider the geometry depicted in Fig. 1. A ballistic sheet of graphene in the (x, y) -plane contains a potential barrier of height V_0 and length d and a superconducting contact in the region $x \geq 0$. The barrier can be implemented by employing the electric field effect [14, 15] via a gate voltage and superconductivity can be induced in the region $x \geq 0$ via the proximity effect. We assume the potential step V_0 to be abrupt on both sides, which is justified close to the Dirac point where the Fermi wavelength $\lambda_F \gg d$ and which can be realized experimentally [15]. The conductance $G(eV)$ through

such a graphene NIS junction has recently been studied, both for potential barriers of finite length [16] and in the limit of a thin barrier [17]. Here we investigate the adiabatically pumped current through the latter junction. The pumped current is induced by periodic variations of $U_0(t) = U_0 + \delta U_0 \cos(\omega t)$ and $V_0(t) = V_0 + \delta V_0 \cos(\omega t + \phi)$. The total pumped current I into the normal lead (the left contact in Fig. 1) can be expressed as an integral over the area A that is enclosed in (U_0, V_0) parameter space during one period, and is given by the scattering matrix expression [8]

$$I \equiv I_N = \frac{\omega e}{2\pi^2} \int_A dU_0 dV_0 \sum_{\alpha, \beta \in N} \Pi_{\alpha\beta}(U_0, V_0) \quad (1)$$

$$\approx \frac{\omega e}{2\pi} \delta U_0 \delta V_0 \sin \phi \sum_{\alpha, \beta \in N} \Pi_{\alpha\beta}(U_0, V_0) \quad (2)$$

with

$$\Pi_{\alpha\beta}(U_0, V_0) \equiv \text{Im} \left(\frac{\partial S_{\alpha\beta}^{ee*}}{\partial U_0} \frac{\partial S_{\alpha\beta}^{ee}}{\partial V_0} - \frac{\partial S_{\alpha\beta}^{he*}}{\partial U_0} \frac{\partial S_{\alpha\beta}^{he}}{\partial V_0} \right). \quad (3)$$

Eq. (2) is valid in the bilinear response regime where $\delta U_0 \ll U_0$ and $\delta V_0 \ll V_0$ and the integral in Eq. (1) becomes independent of the pumping contour. The indices α and β sum over all modes in the normal lead and S denotes the Landauer-Büttiker scattering matrix whose elements $S_{\alpha\beta, nm}^{he}$ describe the scattering of an electron in mode m in lead β to a hole in mode n in lead α .

The low-energy excitations in the NIS junction close to the Dirac point $K(K')$ are described by the 4×4 Dirac-Bogoliubov-deGennes Hamiltonian [13]

$$\mathcal{H} = \begin{pmatrix} \mathcal{H}_a - E_F + U(x) & \Delta(x) \\ \Delta^*(x) & E_F - U(x) - \mathcal{H}_a \end{pmatrix} \quad (4)$$

with $\mathcal{H}_a = -i\hbar v_F(\sigma_x \partial_x + \text{sgn}(a)\sigma_y \partial_y)$, where $\text{sgn}(a)$ is \pm for $a = K(K')$, v_F denotes the Fermi velocity of the quasi-particles, and the potential $U(x) = -U_0\theta(x) + V_0\theta(-x)\theta(x+d)$. The pair potential $\Delta(x)$ which couples the electron and hole excitations has the form $\Delta_0 e^{i\phi}$ and we assume that $(E_F + U_0) \gg \Delta_0$, the mean-field condition for superconductivity. Two regimes can be distinguished: $E_F \gg \Delta_0$ where the usual retro Andreev reflection dominates, and $E_F \leq \Delta_0$ so $U_0 \gg \Delta_0$, where specular Andreev reflection dominates [13]. Our analysis focuses on the retro reflection regime unless we explicitly mention that we study the specular reflection regime. The Hamiltonian (4) acts on the four-component wavefunction $\psi_a = (\psi_{Aa}, \psi_{Ba}, \psi_{A\bar{a}}^*, -\psi_{B\bar{a}}^*)$, where A and B denote the two nonequivalent sides of the graphene unit lattice and $\bar{a} = K'(K)$ for $a = K(K')$. Following Ref. [17], we also introduce the dimensionless barrier strength $\chi = dV_0/(\hbar v_F)$ which allows us to consider the limit of a thin barrier where $V_0 \rightarrow \infty$ and $d \rightarrow 0$ such that χ remains finite.

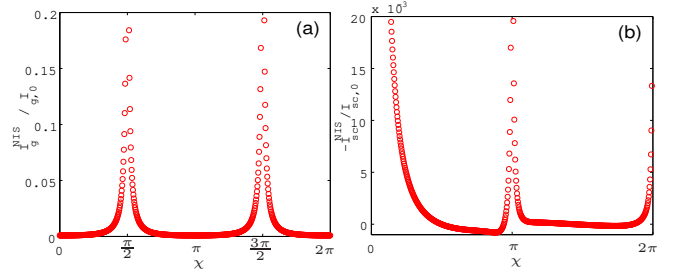


FIG. 2. (a) The pumped current I_g^{NIS} (Eq. (7)) as a function of the potential barrier strength χ in a graphene (g) NIS junction. (b) The analogous pumped current I_{sc}^{NIS} (Eq. (10)) in a semiconductor (sc) NIS junction, where $\sqrt{2mE_F}d/\hbar = 10$.

After applying continuity of the wavefunctions at the boundaries $x = -d$ and $x = 0$, one obtains the reflection and transmission coefficients of the NIS junction, see Eqns. (9) in Ref. [17]. At the Dirac point $\epsilon = 0$, where ϵ denotes the energy of the electrons measured from the Fermi level [18], and defining $\delta = E_F/(E_F + U_0)$, the derivatives of the coefficients for normal and Andreev reflection, r and r_A , with respect to the gate voltages U_0 and V_0 are given by $\partial r_{(A)}/\partial U_0 = (\partial r_{(A)}/\partial \delta)(\partial \delta/\partial U_0)$ and $\partial r_{(A)}/\partial V_0 = (\partial r_{(A)}/\partial \chi)(\partial \chi/\partial V_0)$ with

$$\begin{aligned} \frac{\partial r}{\partial \chi} &= \frac{2e^{i\alpha} \sin \gamma \cos \alpha (\cos 2\chi + \sin \gamma \sin \alpha - i \cos \alpha \sin 2\chi)}{(1 + \sin \gamma \sin \alpha \cos 2\chi)^2}, \\ \frac{\partial r^*}{\partial \delta} &= \frac{-ie^{-i\alpha} \sin \alpha \cos \alpha (\cos 2\chi \cos \alpha + i \sin 2\chi)}{(1 + \sin \gamma \sin \alpha \cos 2\chi)^2}, \\ \frac{\partial r_A}{\partial \chi} &= \frac{-2ie^{-i\phi} \sin \gamma \cos \gamma \sin \alpha \cos \alpha \sin 2\chi}{(1 + \sin \gamma \sin \alpha \cos 2\chi)^2}, \\ \frac{\partial r_A^*}{\partial \delta} &= \frac{-ie^{i\phi} \cos \alpha \sin \alpha (\sin \gamma + \sin \alpha \cos 2\chi)}{\cos \gamma (1 + \sin \gamma \sin \alpha \cos 2\chi)^2}. \end{aligned} \quad (5)$$

Here $\sin \gamma \equiv \delta \sin \alpha$ with α the angle of incidence of the electron. Substituting Eq. (5) into Eq. (2) and integrating over the angle of incidence yields the pumped current at $\epsilon = 0$

$$I_g^{NIS} = I_{g,0} \frac{\delta^2}{\pi} \int_0^{\pi/2} d\alpha \frac{\sin \gamma \sin \alpha \cos^4 \alpha}{(1 + \sin \gamma \sin \alpha \cos 2\chi)^3} \quad (6)$$

$$\stackrel{U_0=0}{=} I_{g,0} \frac{4 \cos^4 \chi - 12 \cos^2 \chi + 8\sqrt{2} |\cos \chi| - 3}{16\sqrt{2} |\cos \chi| (2 \cos^2 \chi - 1)^3} \quad (7)$$

where $I_{g,0} \equiv \omega e \frac{d}{\hbar v_F E_F} \delta U_0 \delta V_0 \sin \phi$. Eq. (7) is valid for $U_0 = 0$. Note from Eq. (6) that there is no contribution to I_g^{NIS} from normally incident electrons with $\alpha = 0$. This is a display of the Klein tunneling effect where the Andreev reflection coefficient $|r_A(\alpha = 0)| = 1$ independent of χ and U_0 .

Figure 2(a) shows the pumped current, Eq. (7), as a function of χ . Notice that I_g^{NIS} , just as the conductance in this system [17], is periodic in χ with a period π . We see that I_g^{NIS} reaches maximum values when $V_0 d = (n + 1/2)\pi \hbar v_F$, where n is an integer. This is the

condition for resonant transmission (i.e., $r = 0$) when the conductance of the system reaches a sharply peaked maximum [17]. Due to the sharp changes in the derivative of r the pumped current diverges at this point. Expanding Eq. (7) with respect to χ around $\chi = 0$, we find that I_g^{NIS} scales as

$$I_g^{NIS}/I_{g,0} \sim a_0 + a_1 \chi^2 \quad (8)$$

where $a_0 = \frac{16-11\sqrt{2}}{32} \approx 0.014$ and $a_1 = 3(1 - \frac{45}{32\sqrt{2}}) \approx 0.017$. The pumped current thus increases with the barrier height close to $\chi = 0$, which is another manifestation of the Klein paradox. Next, we analyze the behavior of the current with respect to U_0 . We expand Eq. (6) with respect to U_0 around $U_0 = 0$ at $\chi = 0$, which results in

$$I_g^{NIS}/I_{g,0} \sim b_0 - b_1 U_0 \quad (9)$$

where $b_0 = a_0$ and $b_1 = \frac{3\sqrt{2}}{128} \approx 0.033$. Eq. (9) shows that the pumped current decreases with increasing U_0 .

Figure 2(b) shows the corresponding pumped current I_{sc}^{NIS} in a *semiconductor* NIS junction. We model the insulating region again as a barrier of height V_0 and width d , and define the dimensionless barrier strength $\chi = \sqrt{2mV_0}d/\hbar$. Solving the Bogoliubov-deGennes equation, matching the wavefunction and its derivative at the boundaries, obtaining r and r_A and calculating the derivatives with respect to the gate voltages V_0 and U_0 yields the pumped current (at the Dirac point $\epsilon = 0$ and for $U_0 = 0$);

$$I_{sc}^{NIS} = I_{sc,0} \int_0^{\pi/2} d\alpha \cos \alpha k^3 d^3 \chi^3 \frac{(2\chi(k^2 d^2 - \chi^2) - (k^2 d^2 + \chi^2) \sin 2\chi)}{(2k^2 d^2 \chi^2 \cos^2 \chi + (k^4 d^4 + \chi^4) \sin^2 \chi)^3}, \quad (10)$$

where $I_{sc,0} \equiv (\omega e/\pi)(2m^2 d^4/\hbar^4)\delta U_0 \delta V_0 \sin \phi$ and $k \equiv (\sqrt{2mE_F}/\hbar) \cos \alpha$. Eqns. (7) and (10) are the main results of this Letter. From Eq. (10) we notice that, in contrast to graphene, the normally incident electrons in the semiconductor junction do contribute to the pumped current, illustrating the absence of Klein tunneling in a semiconductor NIS junction. Figure 2(b) displays I_{sc}^{NIS} as a function of the barrier strength χ . We observe that I_{sc}^{NIS} also oscillates as a function of χ with a period of π . However, the maxima at resonant transmission occur when $\chi = n\pi$ and are thus shifted by $\pi/2$ with respect to the maxima of I_g^{NIS} . Notice that I_{sc}^{NIS} and I_g^{NIS} mostly have opposite signs and that I_{sc}^{NIS} switches sign at several points. In addition, the pumped current in a semiconductor NIS junction is roughly one order of magnitude larger than in graphene [19].

An important question arising when thinking about experimental detection of pumped currents is how to distinguish them from the conductance G in the system. In order to answer this question we explicitly compare both quantities. The conductance of the NIS junction in

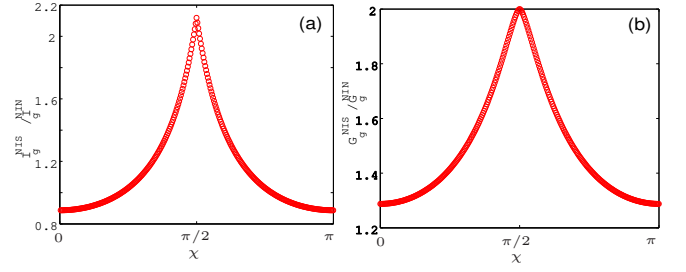


FIG. 3. Ratio of the pumped current (left) and the conductance (right) of the NIS junction and the NIN junction in graphene versus χ for $\epsilon = 0$ and $U_0 = 0$.

graphene was considered in Ref. [17] and is given by, at $\epsilon = 0$ and $U_0 = 0$,

$$G_g^{NIS} = G_0 \frac{\sqrt{A}(A+3) + (A^2 - 2A - 3) \arctan(\sqrt{A})}{A^{5/2}}, \quad (11)$$

where $G_0 \equiv \frac{4e^2}{h} \frac{E_F w}{\pi \hbar v_F}$ with w the width of the sample and $A \equiv \cos 2\chi$. Expanding G_g^{NIS} for small χ around $\chi = 0$ at $U_0 = 0$ and for small U_0 around $U_0 = 0$ at $\chi = 0$ yields, respectively,

$$G_g^{NIS}/G_0 \sim (4 - \pi) + (16 - 5\pi)\chi^2, \quad (12)$$

$$G_g^{NIS}/G_0 \sim (4 - \pi) + (2 - \pi/2)U_0/E_F. \quad (13)$$

We find that $G_g^{NIS} = (4 - \pi)G_0$ for $U_0 = \chi = 0$, somewhat below the ballistic value G_0 due to mismatch in Fermi wavelength in the normal and superconducting leads, as mentioned earlier [13]. Comparing the scaling behavior of G_g^{NIS} and I_g^{NIS} as a function of χ , Eqns. (8) and (12), we find that both transport quantities increase with increasing χ . However when comparing Eqns. (9) and (13) we see that whereas the pumped current I_g^{NIS} decreases with increasing U_0 , the conductance G_g^{NIS} increases with increasing U_0 . Intuitively, switching on U_0 increases the Fermi level mismatch, which increases the conductance [20] however decreases the pumped current. This difference can be used to discriminate the pumped current from the conductance in an actual experiment.

We now investigate the influence of the superconducting lead on the pumped current by comparing I_g^{NIS} with the pumped current I_g^{NIN} through an entirely normal NIN junction in graphene. At the Dirac point $\epsilon = 0$ and for $U_0 = 0$ the latter is given by

$$I_g^{NIN} = I_{g,0} \frac{(1 - |\cos \chi|)^2}{16 |\cos \chi| \sin^4 \chi}. \quad (14)$$

Similarly, the conductance through a NIN junction is given by

$$G_g^{NIN} = G_0 \frac{\sin \chi - \cos^2 \chi \operatorname{arctanh}(\sin \chi)}{\sin^3 \chi}. \quad (15)$$

Figure 3 shows the ratios I_g^{NIS}/I_g^{NIN} and G_g^{NIS}/G_g^{NIN} versus χ . In both cases, the superconducting lead enhances

the transport reaching a maximum at $\chi = \pi/2$. For the conductance this maximum enhancement is 2 due to the contribution of the holes [21], while the enhancement of the pumped current rises from $2(16 - 11\sqrt{2}) \approx 0.89$ at $\chi = 0$ to a factor of $3\sqrt{2}/2 \approx 2.12$ at $\chi = \pi/2$. However, when comparing I_g^{NIS} (Eq. (6)) and I_g^{NIN} per mode at $\chi = \pi/2$, i.e., before integration over α , we see that the superconducting lead enhances the pumped current of each mode by a factor of 4. This last result is due to both the holes which contribute a factor of 2 and the asymmetry of the NIS junction with respect to injection of charge carriers which contribute another factor of 2 [8].

At this point we briefly mention the behavior of the pumped current as a function of an applied bias voltage eV both in the normal (retro) and in the specular Andreev reflection regime [22]. For bias voltages below the gap $eV \leq \Delta_0$, the pumped current I_g^{NIS} in the retro reflection regime decreases from a finite value at $eV = 0$ (see Eq. (7)) to zero at $eV = \Delta_0$. At $eV = \Delta_0$, the particles are fully Andreev reflected ($|r_A| = 1$ independent of χ and U_0) and therefore $I_g^{NIS} = 0$. In the specular reflection regime [13] where $E_F \leq \Delta_0$ and $U_0 \gg E_F$, the pumped current exhibits different behavior. First, the pumped current, just as the conductance [17], is insensitive to χ for energies below the gap. The large mismatch in Fermi energies of the normal and the superconducting leads already acts as a barrier, and as a result the addition of another barrier is irrelevant, explaining this behavior. Furthermore, the pumped current I_g^{NIS} is zero for bias voltages equal to the Fermi level $eV = E_F$, due to the absence of Andreev reflection [13], and also for $eV = \Delta_0$, see the discussion above. As a final remark, the pumped current is several orders of magnitudes smaller than in the retro reflection regime.

Finally, we briefly comment on possibilities for experimental observation of our predictions. Experiments with superconducting electrodes on top of graphene in which multiple Andreev reflections were observed have already been carried out [23, 24]. From these experiments we can estimate the order of magnitude of the pumped current. Some typical parameters are $\omega/(2\pi) = 5$ GHz, $E_F = 80$ meV, $v_F = 10^6$ m/s and barrier width $d = 10 - 20$ nm [15, 25]. For gate voltages on the order of 10 meV, the pumped current is on the order of 10 fA far from the resonant tunneling condition, going up to 0.1 – 1 pA or higher close to resonance.

In conclusion, we have investigated adiabatic quantum pumping in a graphene NIS junction, which is generated by periodic modulation of the insulating barrier V_0 and the Fermi level on the superconductor side. We have demonstrated that the presence of the superconducting lead can enhance the pumped current per mode by a factor of 4 (at resonance) and suggested experimentally observable differences between the conductance and the

pumped current in this system.

This work has been supported by the Netherlands Organization for Scientific Research (NWO/FOM).

-
- [1] M. Büttiker, H. Thomas, and A. Prêtre, Z. Phys. B **94**, 133 (1994).
 - [2] P. W. Brouwer, Phys. Rev. B **58**, 10135 (1998).
 - [3] B. Spivak, F. Zhou, and M. T. Beal-Monod, Phys. Rev. B **51**, 13226 (1995).
 - [4] M. Switkes *et al.*, Science **283**, 1905 (1999); E. R. Mucciolo, C. Chamon, and C. M. Marcus, Phys. Rev. Lett. **89**, 146802 (2002); P. Sharma and P. W. Brouwer, Phys. Rev. Lett. **91**, 166801 (2003); S. K. Watson *et al.*, Phys. Rev. Lett. **91**, 258301 (2003).
 - [5] J. E. Avron *et al.*, Phys. Rev. B **62**, R10618 (2000).
 - [6] See e.g.; J. Splettstoesser *et al.*, Phys. Rev. Lett. **95**, 246803 (2005); E. Sela and Y. Oreg, Phys. Rev. Lett. **96**, 166802 (2006); F. Reckermann, J. Splettstoesser, and M. R. Wegewijs, Phys. Rev. Lett. **104**, 226803 (2010).
 - [7] J. Wang *et al.*, Appl. Phys. Lett. **79**, 3977. (2001).
 - [8] M. Blaauboer, Phys. Rev. B **65**, 235318 (2002).
 - [9] F. Taddei, M. Governale, and R. Fazio, Phys. Rev. B **70**, 052510 (2004).
 - [10] M. Governale, F. Taddei, R. Fazio, and F. W. J. Hekking, Phys. Rev. Lett. **95**, 256801 (2005).
 - [11] J. Splettstoesser *et al.*, Phys. Rev. B **75**, 235302 (2007).
 - [12] E. Prada, P. San-Jose, and H. Schomerus, Phys. Rev. B **80**, 245414 (2009); R. Zhu and H. Chen, Appl. Phys. Lett. **95**, 122111 (2009); E. Prada, P. San-Jose, and H. Schomerus, (2010), arXiv:1007.3161; G. M. M. Wakker and M. Blaauboer, Phys. Rev. B **82**, 205432 (2010).
 - [13] C. Beenakker, Phys. Rev. Lett. **97**, 067007 (2006).
 - [14] K. S. Novoselov *et al.*, Science **306**, 666 (2004).
 - [15] M. I. Katsnelson *et al.*, Nature Phys. **2**, 620 (2006).
 - [16] S. Bhattacharjee, M. Maiti, and K. Sengupta, Phys. Rev. B **76**, 184514 (2007).
 - [17] S. Bhattacharjee and K. Sengupta, Phys. Rev. Lett. **97**, 217001 (2006).
 - [18] We remark that $\epsilon = 0$ is the point of highest interest for observing quantum pumping, since it corresponds to the situation in which no bias voltage is applied.
 - [19] Here we used that $I_{sc}^{NIS} = I_g^{NIS}(2mE_F)^{3/2}d^3/(\pi\hbar^3)$.
 - [20] See also Ref. [13], where it was assumed that $U_0 \gg E_F$. The conductance is then given by $G = (4/3)G_0$ at zero bias $eV = 0$ and decreases to the value $G = (4 - \pi)G_0$ for $eV \gg \Delta_0$, in which case the Fermi level mismatch is minimal.
 - [21] C. W. J. Beenakker, *Mesoscopic quantum physics*, edited by E. Akkermans, G. Montambaux, J.-L. Pichard, and J. Zinn-Justin (North-Holland, Amsterdam, 1995) see also cond-mat/9406083.
 - [22] A more extensive analysis is in preparation and will be published elsewhere.
 - [23] H. B. Heersche *et al.*, Nature **446**, 56 (2007).
 - [24] F. Miao *et al.*, Science **14**, 1530 (2007).
 - [25] K. S. Novoselov *et al.*, Nature **438**, 197 (2005); Y. Zhang *et al.*, *ibid.* **438**, 201 (2005); K. S. Novoselov *et al.*, Nature Physics **2**, 177 (2006).